KSME

Springer

Journal of Mechanical Science and Technology 34 (1) 2020

Original Article
DOI 10.1007/s12206-019-1231-z

Keywords:
· Shearing
· Shaving
· Cutting
· Steel
· Strength
· Crack

Correspondence to:
Sutasn Thipprakmas
sutasn.thi@kmutt.ac.th

Citation:
Thipprakmas, S., Sontamino, A. (2020). Fabrication of clean cut surface on high-strength steel using a new shaving die design. Journal of Mechanical Science and Technology 34 (1) (2020) 301-317.
http://doi.org/10.1007/s12206-019-1231-z

Received March 6th, 2019
Revised October 4th, 2019
Accepted October 25th, 2019

† Recommended by Editor Hyung Wook Park

Fabrication of clean cut surface on high strength steel using a new shaving die design

Sutasn Thipprakmas and Arkarapon Sontamino

Dept. of Tool and Materials Engineering, King Mongkut's University of Technology Thonburi, Bangkok, Thailand

Abstract A shaving process is commonly applied to achieve a smooth cut surface thorough the workpiece thickness and a square cut-edge, also known as a finishing operation. However, this process is rarely successful for high-strength steel sheets, which is a major problem. In the present study, finite element method (FEM) simulation was used to clarify the main causes of this problem by comparing the shaving mechanisms between medium carbon steel grade SPCC (JIS) and high-strength steel grade SPFH 590 (JIS). Results show that in the case of SPFH 590 based on material flow, stress distribution, and strain distribution analyses, the shaved chip was difficult to form by sliding along the punch face. Moreover, the tensile stress generated in the shearing zone was increased and readily generated cracks. The shaving process was developed in the present study by generating the cutting-edge angle and rake radius on the punch. The cutting edge angle was designed to generate high compressive stress in the cutting-edge vicinity and shearing zone, and the rake radius was designed to tear a shaving allowance off and move it along the rake radius instead of moving downward along the punch movement direction, thereby decreasing the tensile stress in the shearing zone. Under these mechanisms, the increases in the generated tensile stress in the shearing zone could be delayed, and cracks could thus be prevented. The effect of the punch geometry on the cut surface characteristics and cutting forces were also investigated. Laboratory experiments were performed to validate the FEM simulation results. Experimental results agreed well with the FEM simulation results. Therefore, a smooth cut surface thorough the workpiece thickness of high-strength steel sheets could be successfully achieved by using the developed shaving process.

1. Introduction

In recent years, metal die cutting processes, such as shearing, blanking, trimming, and fineblanking, have been developed by many researchers and engineers to achieve improved dimensional accuracy of cut surface characteristics and increase process efficiency [1-16]. These processes are commonly applied in many industrial fields, including the automobile industry, electronics, and medical equipment industries, in which strict requirements on dimensional part accuracy are specified. Computer technologies for engineering problems have greatly progressed in recent years, and many studies have been conducted based on these technologies. A neural expert system for the condition-based maintenance of blanking has been proposed to detect tool wear and other important aspects of the punching and blanking processes by monitoring force-displacement measurements [1]. A combination of the finite element method (FEM) and artificial neural networks, as a new approach, has been proposed to help reduce the simulation time and enable searching for the optimal process parameters in fine blanking [2].

Computer-aided process planning has been considered to be combined with computer-aided design and computer-aided manufacturing (CAM) for sheet metal blanking die design and

Table 1. FEM simulation and experimental conditions.

Simulation model				Plane strain model
Object type				Workpiece: Elastoplastic Punch, die, blank holder: Rigid
Workpiece material	SPFH 590			Tensile strength (δ_u): 615 MPa Elongation (δ): 26 % Young's modulus (E): 203000 MPa Poisson's ratio (v): 0.33
	SPCC			Tensile strength (δ_u): 346 MPa Elongation (δ): 47 % Young's modulus (E): 208000 MPa Poisson's ratio (v): 0.33
Flow curve equation	SPFH 590			$\bar{\sigma} = 969.20\varepsilon^{0.15} + 481$
	SPCC			$\bar{\sigma} = 554.43\varepsilon^{0.23} + 208$
Fracture criterion equation	SPFH 590	Shearing process		Ayada
		Shaving process	Conventional die	Ayada
			Proposed die	Normalized Cockroft-Latham
	SPCC	Shearing process		Normalized Cockroft-Latham
		Shaving process		Normalized Cockroft-Latham
Critical fracture value	SPFH 590	Shearing process		0.60
		Shaving process	Conventional die	0.60
			Proposed die	0.80
	SPCC	Shearing process		2.08
		Shaving process		2.08
Workpiece geometry				Thickness (t): 2 mm
				Length (WP_L): 80 mm
				Width (WP_W): 20 mm
Friction coefficient (μ)				0.1
Shearing clearance (Cl)				1 %t, 5 %t, 15 %t, 25 %t
Shaving allowance (D_{sh})				0.1, 0.3, 0.5, 1.0 mm
Proposed shaving-punch geometry				Cutting edge angle (Θ_C): 20°, 30°, 40°
				Cutting edge width (C_w): 0.5, 0.8, 1.0 mm
				Rake radius (R_r): 2, 4, 6 mm
				Cutting-edge radius: Sharp edge

manufacturing [8]. Many studies have used FEM to investigate the effects of process parameters and develop die designs. Lo et al. [3] investigated the effects of punch materials, cutting clearance, shear angle, and number of shearing strokes on smooth cut surface and die roll. Sontamino and Thipprakmas [10] compared the cut surface features in various die cutting processes, including shearing, blanking, and punching processes. A new die design achieved by chamfering the cutting edge in a fine-piercing process has been proposed using FEM techniques [4]. A punch with an inclined edge has also been proposed for sheet metal blanking process [12]. Many studies based on experiments have also been conducted [5-7]. Peter et al. [5] investigated the temperature distribution in the shearing zone during sheet metal blanking process. A piezoelectric-based nondestructive method has been applied to monitor the contact pressure on the sheet near the cutting edge during fineblanking. The maximum contact pressure appears at the beginning of sheet punching [7].

In recent years, high-strength steel has been one of the most effective examples of leading-edge applications in high-performance material uses, and it is increasingly applied in modern automobiles for weight reduction and fuel savings. The material used in the present study is high-strength steel grade SPFH 590 (JIS). The material is widely used to fabricate many automobile parts, such as members/pillars, subframes, and front-end carriers. This material is a high-strength steel with a microstructure composed of ductile ferrite and high-strength martensite produced by thermomechanical processing. The tensile strength and ductility of various high-strength steels are varied with the volume fraction of the martensite phase. These steels have high strength but low formability. Therefore, given its high strength, cutting by die cutting and achieving accurate cut parts is quite difficult. Specifically, when applying a large cutting clearance [17-20], the cut-edge characteristic with a

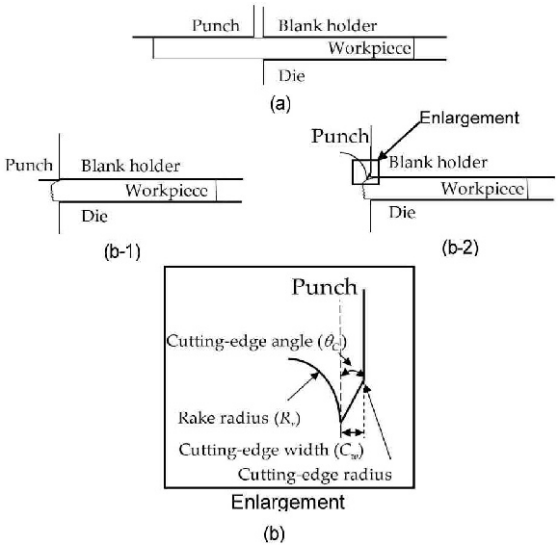

Fig. 1. FEM simulation models of the shaving process: (a) Shearing operation; (b) shaving operation: (b-1) Conventional shaving die; (b-2) proposed shaving die.

poorly square cut-edge is formed, in addition to a large die roll and small smooth surface. By contrast, when using a smaller cutting clearance [21-23], a smooth surface with a tearing defect is generated, although the die roll and poorly square cut edge is reduced. These characteristics are the major defects of the cut edge, and they degrade the quality of the cut parts. These factors motivate the need for secondary operations for which production costs and time requirements are increased. To solve these problems, many studies have been conducted based on experiments and FEM techniques [24-29]. Hongli et al. [24] studied the effects of process parameters on the microstructure and accuracy of B1500HS steel parts in hot blanking and blanked parts with high-dimensional accuracy, improved mechanical properties, and wear resistance at blanking temperatures of 750 °C-800 °C. A punching technique with a slight clearance using a punch with a small round edge has been developed to delay cracks and improve the quality of sheared edge for ultra-high strength steel sheets [25]. A new simulation model based on the utilization of the damage zone and a new parameter, the effective failure strain ratio, has been proposed to improve the prediction of the edge stretchability of DP780 [28]. However, no studies have demonstrated the fabrication of a smooth cut surface thorough the workpiece thickness. Therefore, smooth cut surface thorough the workpiece thickness is the main target of the present study to increase the accuracy of cut parts.

A shaving process is usually considered a finishing operation in a metal die cutting process to achieve improved dimensional accuracy of cut surface characteristics by obtaining smooth cut surface and square cut edge thorough the workpiece thickness. Although many previous studies have been conducted to clarify the shaving mechanism and increase the accuracy of shaved parts, nearly all such studies have been conducted on conventional material types, such as carbon steel and aluminum alloy sheets [13-16]. Therefore, in the present study, the developed shaving process for high-strength steel sheets was proposed to obtain a smooth cut surface thorough the workpiece thickness. The concept of this development was clarified by making the cutting-edge angle and rake radius on the punch. In addition, the effect of the punch geometry on shaved surface characteristics, including cutting-edge angle, cutting-edge width, and rake radius, was also investigated. FEM simulation based on material flow and stress distribution analyses was used to clarify the shaving mechanisms of the developed shaving process and the effect of the punch geometry on cut surface characteristics. Laboratory experiments were also conducted to validate the FEM simulation results. FEM simulation results indicated good agreement with the experimental results in terms of cut surface characteristics and cutting forces. These results show that the fabrication of smooth cut surfaces thorough the material thickness of high-strength steel sheets could be performed by the developed shaving process with suitable dimensions of cutting-edge angle, cutting-edge width, and rake radius.

2. Materials and methods

In the present study, the principles of the shaving process and the investigated models for conventional and developed shaving processes are illustrated in Fig. 1. First, the workpiece is sheared; this step is called the shearing operation, as shown in Fig. 1(a). Next is the conventional shaving operation (Fig. 1(b-1)) and the developed shaving operations with the new punch model (Fig. 1(b-2)). With the shaving operation, the sheared workpiece is again placed on the die and is cut with a shaving allowance away from an already sheared workpiece by setting a zero shaving clearance. Table 1 lists the FEM and experimental details of the models and the process parameters.

On basis of the principles of shearing and shaving processes, in which the workpiece is cut in a straight line, a two-dimensional plane strain with a thickness of 2 mm is applied for the FEM simulation. The physical problem of metal-forming processes in nature is generally considered with quasi-static analysis, in which time dependence is sufficiently slow, such that its inertial effect is negligible. Next, the implicit method is suitably useful in these problems, in which the time dependency of the solution is not an important factor and inertia effects can be neglected. Therefore, in the present study, two-dimensional, implicit, quasi-static analysis is performed with the commercial analytical code DEFORM-2D. The solution algorithm applied to these FEM models is based on the Newton-Raphson iteration. The punch, die, and blank holder are set as rigid types, and the workpiece material is set as an elasto-plastic type. As per previous studies [14-16, 30, 31], approximately 5000 elements based on a four-node rectangular element type have been created for the workpiece to prevent divergence of the calculation due to excessive deformation of the elements during the cutting stage. A fine element region is also generated in the cutting zone, and an adaptive remeshing

technique is applied. On the basis of the accuracy of the FEM simulation result and calculation time, the number of remeshing processes is determined every three steps [14-16, 30, 31]. The plastic properties of the workpiece are assumed to be isotropic and described by the von Mises yield function.

In the present study, as a base material for comparison with the high-strength steel material, medium carbon steel, grade SPCC (JIS), is used as the workpiece material. Next, high-strength steel, grade SPFH 590 (JIS) is used as the representative high-strength steel material for the shaving process. The two types of SPCC and SPFH590 materials are described with an elastoplastic, power-exponent, and isotropic hardening model. As per previous studies [14, 15], the constitutive equations are determined from the stress-strain curve using tensile test, as listed in Table 1. Other necessary material properties are also presented in Table 1. On the basis of the contact surface model defined by a Coulomb friction law [14, 15], a friction coefficient (μ) of 0.10 is applied. Furthermore, the fracture criterion is considered in facilitating crack formation. As per previous studies, the normalized Cockroft-Latham equation is investigated for SPCC [32-35], and the Ayada equation is investigated for SPFH590. On the basis of shearing and shaving processes, the results show agreement between the FEM simulation and the experimental results. Therefore, the normalized Cockroft-Latham equation with a critical fracture value is applied for SPCC, and the Ayada equation with a critical fracture value is applied for SPFH590 (Table 1). This critical fracture value agrees well with the cut surface characteristics in the shearing and shaving processes between the FEM simulation results and the results obtained from the experiments.

In the present study, experiments are conducted to validate the FEM simulation results. On the basis of plane strain condition, a workpiece width of 20 mm is used, and the ratio of workpiece width to thickness is 10. Given this ratio, the cutting deformation under plane strain conditions is primarily controlled. Shearing clearances of 5 %t and 15 %t are applied as recommended for SPCC and SPFH590, respectively. Smaller and larger shearing clearances compared with the recommended clearances are also investigated. Next, the shaving allowances of 0.1, 0.3, and 0.5 mm are applied for SPCC and SPFH590. Figs. 2(a) and (b) show the die set assembled on the press machine in the cases of the conventional and developed shaving process used for the experiments, respectively. A 5 t universal testing machine (Lloyd Instruments Ltd.) is used as the press machine, as shown in Fig. 2.

Five samples from each cutting condition are produced to characterize the obtained cut surface features. The cut surface characteristics, including die roll, smooth cut surface, and crack formation, are measured using a profile projector (Mitutoyo model PJ-A3000). The smooth cut surface and crack formation are measured in three locations on the front view of the cut edge, as shown in Fig. 3(b). Next, the cut parts are cut along the cutting line, labeled in Fig. 3(a), using a wire electrical discharge machining technique. The die roll is measured on the cross section of the cut edge, as shown in the diagram in Fig. 3(c). On the basis of the five samples, the average amounts of die roll, smooth cut surface, and crack formation are calculated, reported, and compared with those determined by the FEM simulations. Then, these cut edges are captured as cut surface characteristic images.

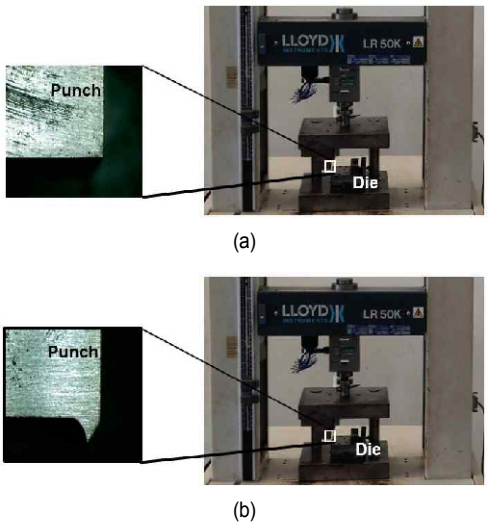

Fig. 2. Die-set for experiments: (a) Conventional shaving die application; (b) proposed shaving die application.

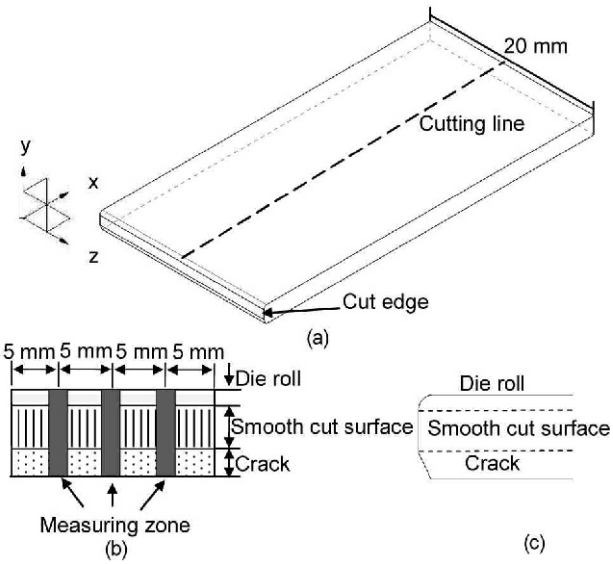

Fig. 3. Illustration of dimension measurements: (a) Cut part; (b) front view (plane yz); (c) cross section (plane xy).

3. Results and discussion

Tables 2 and 3, with respect to the shearing clearances and shaving allowances, show the cut surface characteristics of SPFH590 and SPCC, respectively. In the case of SPFH590, the investigated shearing clearance range was 10-20 %*t*, and the shearing clearance being 15 %*t* was used in the present study [17-20]. In addition, the smaller shearing clearance of

5 %*t* and larger shearing clearance of 25 %*t* compared with the recommended shearing clearance were investigated. The smooth cut surface increased, and crack formation decreased as the shearing clearance increased. In addition, the squareness of the cut edge decreased as the shearing clearance increased. These methods of smooth cut surface, crack formation, and squareness of the cut-edge agreed well with shearing theory and the literature [27, 35]. Next, the shaved surface is shown in Table 2(b).

The results showed a somewhat constant smooth cut surface as the shaving allowance increased. However, as the shaving allowance increased, the die roll and crack formations decreased and increased, respectively. The results also showed that the small shearing clearance with a small shaving allowance produced the obtained large smooth cut surface. These cut surface characteristics agreed well with shaving theory and the literature [27, 35]. However, no successful cases achieved a smooth cut surface thorough the workpiece thickness. In terms of SPCC, the sheared surface characteristics agreed well with shearing theory [35], such that the smooth cut surface and squareness of the cut surface decreased, and crack formation increased with the shearing clearance (Table 3(a)). Again, the shaved surface characteristics agreed well with shaving theory [35], such that the smooth cut surface deceased as the shaving allowance increased (Table 3(b)). From these results, although the cut surface characteristics in the case of SPFH590 agreed with shaving theory and the literature [27, 35] and corresponded well with those obtained in the case of SPCC, a successful smooth cut surface thorough the workpiece thickness could not be obtained. On the basis of these results, the shaving process has been critically limited to applications for SPFH590. Table 4 shows a comparison of the material flow and stress distribution analyses during shaving operation between SPCC and SPFH590. A punch stroke of 0.67 mm, based on shaving theory, was used, and the shaved chip was formed by moving along the punch face. However, given that the yield strength and elongation of the SPCC were lower and higher than those of SPFH590, respectively, the shaved chip was more easily formed by sliding along the punch face in the case of SPCC than in the case of SPFH590 (Tables 4(a-1) and 4(a-3)). The angles of velocity were 24° and 19° in the cases of SPCC and SPFH590, respectively. With this material flow characteristic, the compressive stress was generated in the shaved chip underneath the punch face, and the tensile stress was generated in the cutting-edge vicinity, as shown in Tables 4(a-2) and 4(a-4) for the case of SPCC and SPFH590, respectively. The generated compressive stress in the shaved chip for the case of SPCC was smaller than that in the case of SPFH590, and the tensile stress generated in the cutting-edge vicinity in the case of SPCC was smaller than that in the case of SPFH590. When the punch stroke was increased to 1.14 mm, the material flow analysis showed the same behavior as the previous punch stroke. Specifically, the shaved chip was more easily moved along the punch face in the case of SPCC than in the case of SPFH590, as shown by the angle of velocity in Tables 4(b-1) and 4(b-3), respectively. On the basis of these material flow characteristics, the increases in the compressive stress generated in the shaved chip underneath the punch face and the tensile stress generated in the cutting-edge vicinity are illustrated, as shown in Tables 4(b-2) and 4(b-4) for the cases of SPCC and SPFH590, respectively. For the case of SPFH590, the increase in tensile stress generated in the cutting-edge vicinity was greater than the fracture stress of the material, and the initial crack was formed. By contrast, a crack was not formed in the case of SPCC. For the case of SPCC, this result was in good agreement with shaving theory and the literature [15, 16, 35]; that is, during the shaping phase of the shaving operation, the crack could not be formed, and a smooth cut surface could be achieved. For the case of SPFH590, the opposite was true; this result was in contrast to shaving theory and the literature [15, 16, 35]. This result confirmed that the principle underlying the shaving process could not be used to clarify the shaving mechanism of SPFH590 and that crack formation could not be delayed. At the end of the shaping phase of the shaving operation (Table 4(c)), the material flow analysis showed that the movement of the shaved chip along the punch face was turned toward the direction of the punch movement and directed to the die in the cases of SPCC and SPFH590, as shown in Tables 4(c-1) and 4(c-3), respectively. Given this material flow characteristic, the tensile stress generated in the cutting-edge vicinity and shearing zone slightly decreased for the case of SPCC (Table 4(c-2)). By contrast, the tensile stress generated in the shearing zone was similar to that in the previous punch stroke, and a crack was continuously formed for the case of SPFH590 (Table 4(c-4)). During the shearing phase (Table 4(d)), the results showed that the shaved chip was completely forced to move downward in the direction of the punch movement in the case of SPCC (Table 4(d-1)), and the tensile stress generated in the shearing zone was again increased (Table 4(d-2)). The increase in tensile stress generated in the shearing zone was greater than the fracture stress of the material, and an initial crack was formed. These results of material flow and stress distribution analyses corresponded well with shaving theory and the literature [15, 16, 35]. For the case of SPFH590, the same behavior as the SPCC case could be observed. The shaved chip was continuously forced to move downward in the direction of the punch movement (Table 4(d-3)), and the tensile stress generated in the shearing zone continuously increased as the crack continuously formed (Table 4(d-4)). After the shaving operation, given the shaved surface characteristics shown in Table 4(e), a larger smooth cut surface and smaller crack formation could be obtained in the case of SPCC. The causes of crack formation and the limitation of the shaving process applied for SPFH590 were also clearly characterized. In addition, the cutting mechanism of the shaving process for SPFH590 was demonstrated against the shaving theory. The FEM simulation results were validated by experimental results. The FEM simulation results indicated good agreement of the predicted cut surface characteristics with the experimental results in the cases of SPCC

Table 2. Illustration of sheared and shaved surface characteristics of SPFH 590 with respect to shearing clearance.

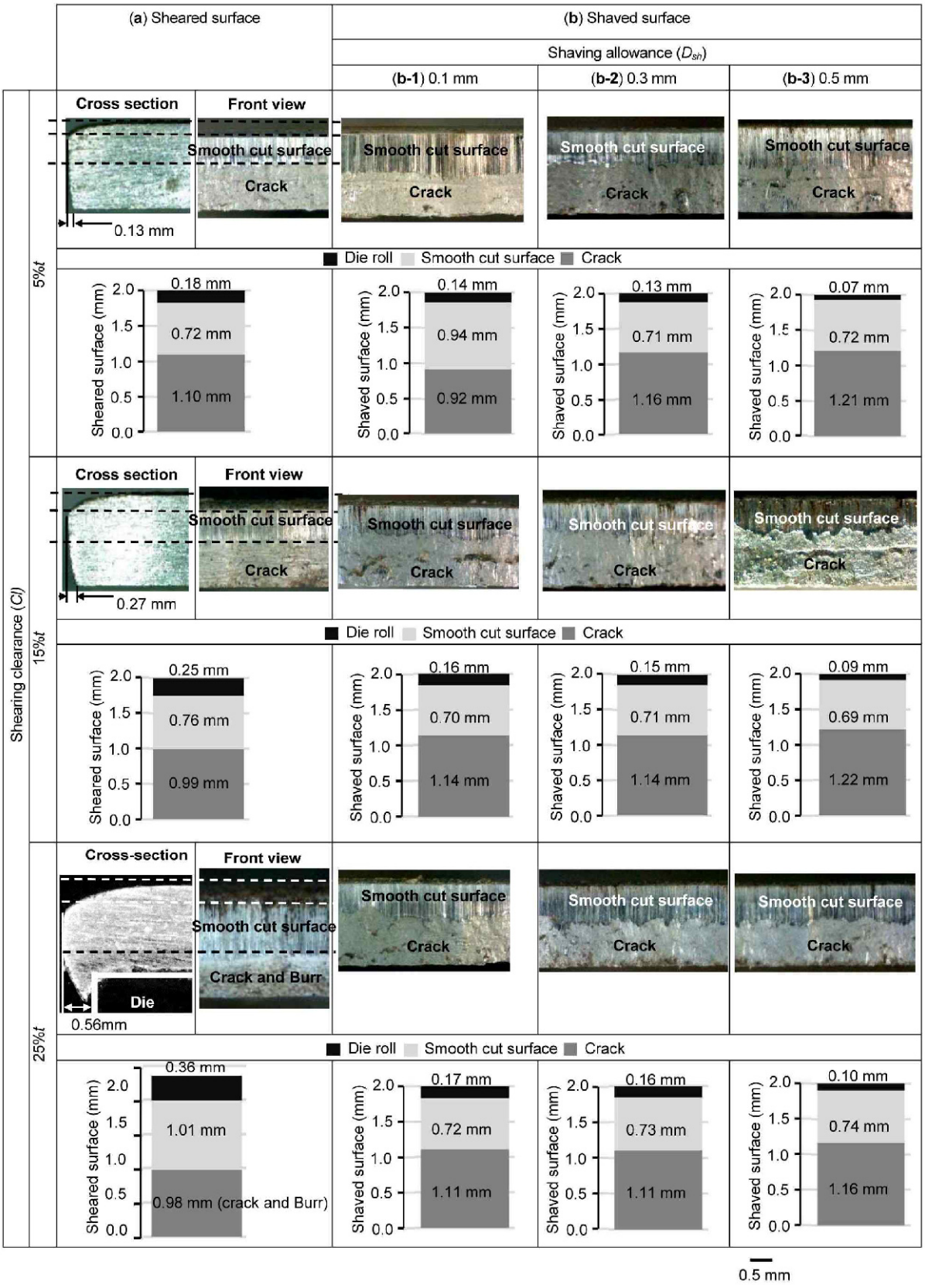

Table 3. Illustration of sheared and shaved surface characteristics of SPCC with respect to shearing clearance.

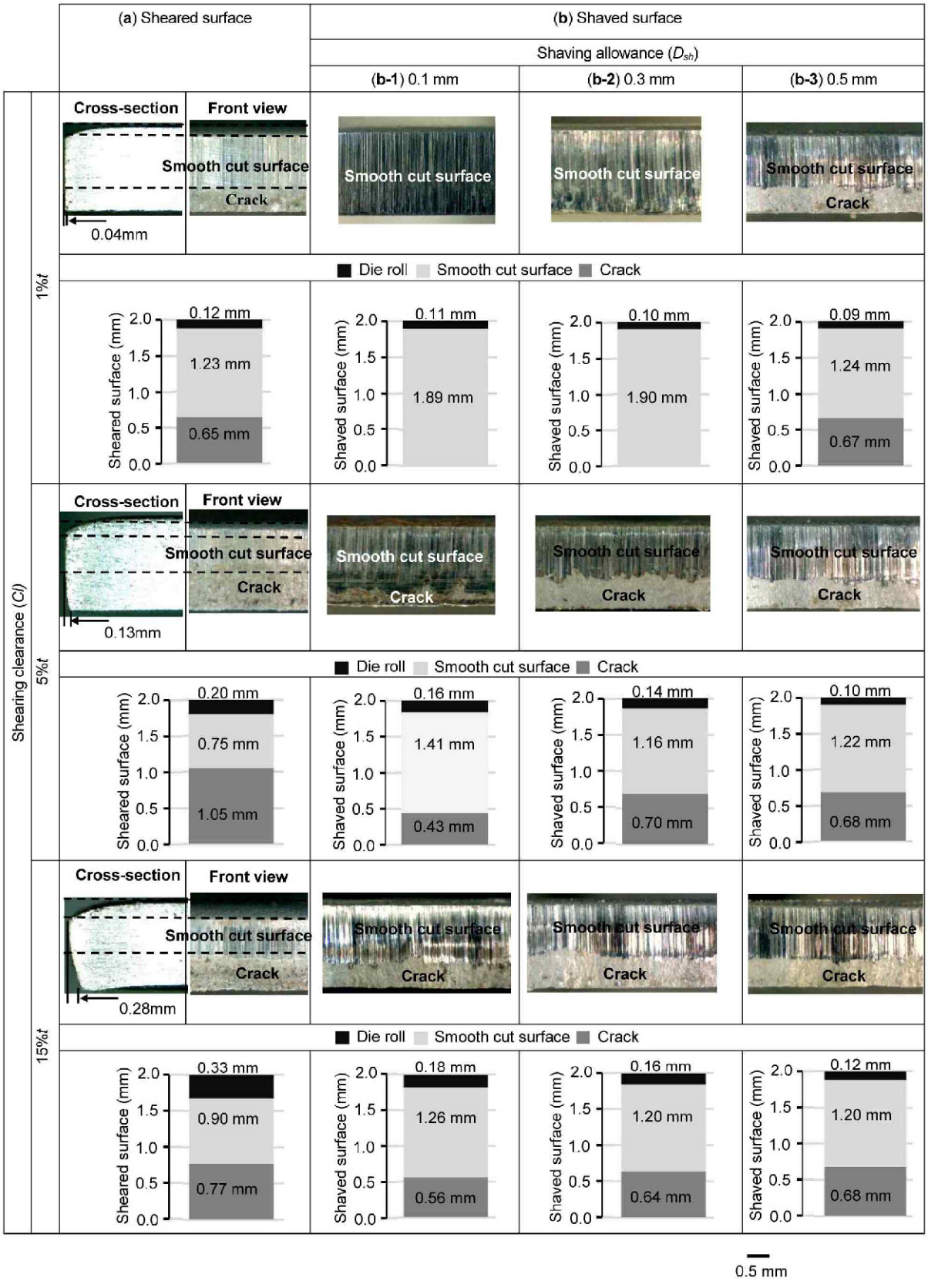

Table 4. Comparison of material flow and stress distribution analyses during shaving operation between SPCC and SPFH590.

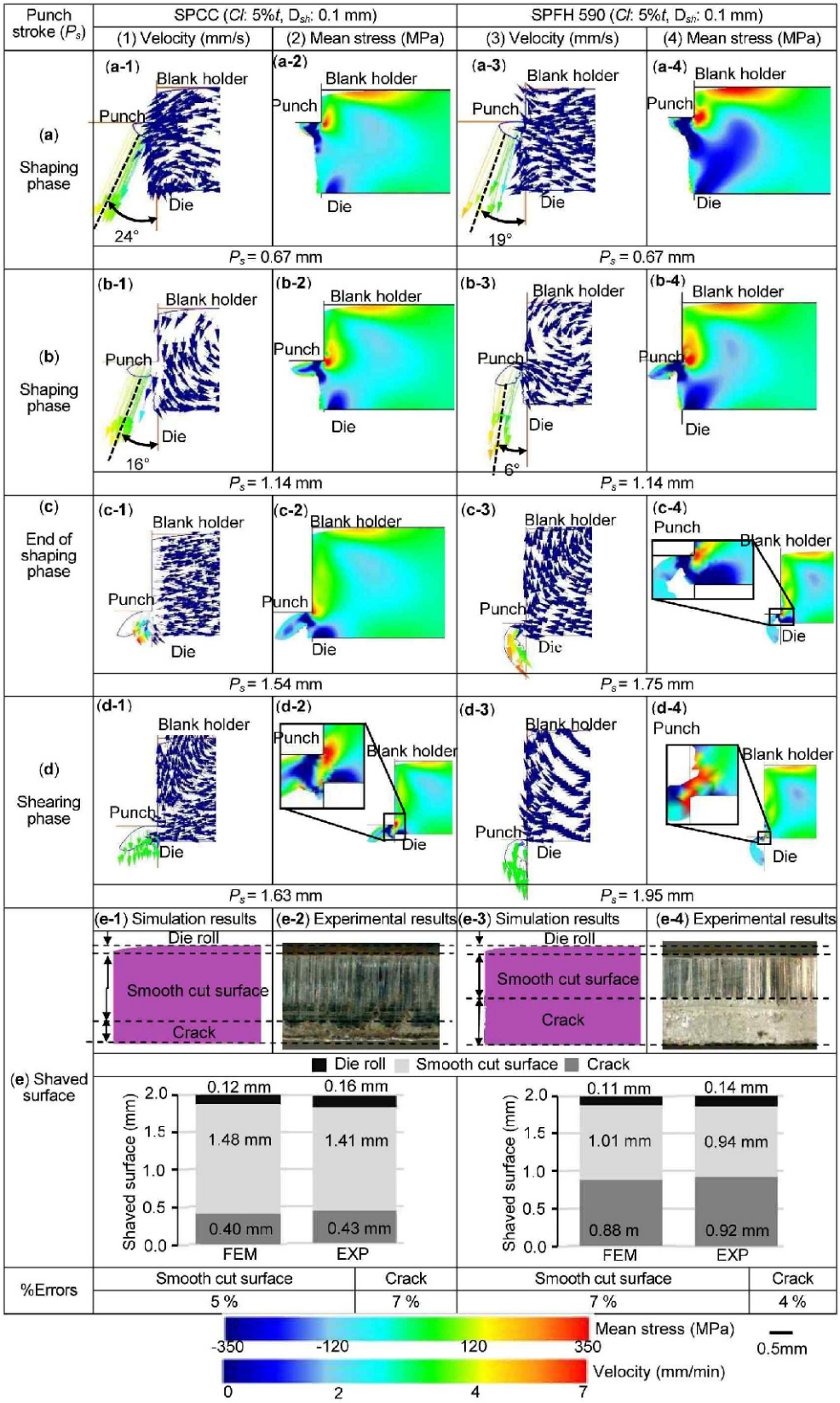

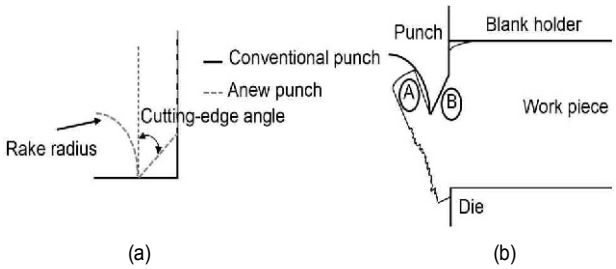

Fig. 4. Illustration of the proposed shaving die design and its principles: (a) Comparison of conventional and proposed shaving die designs; (b) principle of shaving die design.

and SPFH590 (Table 4(e)). The die roll, smooth cut surface, and crack were also measured and reported. The errors of the FEM simulation compared with the experimental results in terms of the smooth cut surface and crack formation were generally less than 7 % in both cases SPCC and SPFH590 cases.

In the present study, on the basis of the aforementioned causes of crack formation and the limitation of the shaving process applied for SPFH590, the shaving process was developed (Fig. 4). The proposed punch (Fig. 4(a)) was designed by making the cutting-edge angle and rake radius. On the basis of the cutting principle of the proposed punch shown in Fig. 4(b), the shaving allowance was separately torn off (zone A) by the rake radius. This torn off shaving allowance was moved along the rake radius instead of downward along the punch movement direction; this process also caused the shaved chips to be smaller. To decrease the high tensile stress generated in the cutting edge vicinity [4], the cutting edge angle analyzed in Fig. 4(b) could prevent the increases in the tensile stress in the shearing zone by generating high compressive stress near the cutting-edge vicinity and shearing zone (zone B). For these behaviors, the tensile stress generated in the cutting-edge vicinity and shearing zone could be decreased, and crack formation could be delayed. Therefore, the shaving process could be successfully conducted for SPFH590 to achieve a smooth cut surface thorough the workpiece thickness. Table 5 shows a comparison of the material flow and stress distribution analyses during shaving operation between the conventional and developed shaving processes. To validate the FEM simulation results, the experimental results were compared with those of FEM simulation results (Table 5). With a punch stroke of 0.60 mm, the material flow analysis showed that the shaving allowance was moved downward by the punch, with a slight movement along the punch face, and a shaved chip was formed, as shown in Table 5(a-1). On the basis of the material flow analysis, as the shaved chip formed, the compressive stress was largely generated underneath the punch face and was decreased and directed to the die side (Table 5(a-2)). By contrast, tensile stress was generated in the punch cutting-edge vicinity and shearing zone. The stress decreased and was directed to the die cutting-edge vicinity (Table 5(a-2)).

These results showed that crack formation readily occurred at the punch cutting edge and directed to the die cutting edge. These results of the material flow, stress distribution, and strain distribution analyses corresponded well with shaving theory and the literature [15, 16, 35]. For the developed shaving process, the shaving allowance was partially cut and was moved downward along the rake radius, as in the material flow analysis shown in Table 5(b-1). These methods of material flow analysis caused the tensile stress to be largely generated on the rake tip, as shown in Table 5(b-2). Given that the shaved chip was pressed to make contact with the die side by cutting-edge width and the compressive stress was formed, the generated tensile stress on the cutting-edge angle was compensated with the compressive stress and then became smaller than that generated on the rake radius. In addition, the cutting-edge angle caused the remainder of the shaving allowance to be partially forced to flow into the shearing zone, as shown in the material flow analysis in Table 5(b-1). Again, this manner of material flow analysis caused the generated compressive stress in the punch cutting-edge vicinity and shearing zone. However, on the basis of shearing theory, the tensile stress was generated in the die cutting-edge vicinity (Table 5(b-2)). Moreover, the propagation of the generated tensile stress on the die cutting edge was directed toward the shaved chip (Table 5(b-2)). By contrast, in the case of the conventional shaving process, the generated tensile stress was directed toward the opposite cutting edge (Table 5(a-2)). The tensile stress was generated in the punch cutting-edge vicinity and shearing zone in the case of conventional shaving process. By contrast, the compressive stress was generated in the punch cutting-edge vicinity and shearing zone in the case of the developed shaving process. The maximum tensile and compressive stresses generated in the shearing zone were approximately 664 MPa and 1980 MPa in the cases of the conventional and developed shaving processes, respectively. This behavior could again be explained by the compensation of the tensile stress generated in the shearing zone with the compressive stress generated near the shearing zone in the case of the developed shaving process, whereas it was not generated in the case of the conventional shaving process.

For the strain distribution analysis, the FEM simulation results showed that in the same manner as the stress distribution analysis, a large strain was generated in the tool cutting-edge vicinity and it was decreased and directed toward the opposite side of the tool cutting-edge vicinity in the case of the conventional shaving process (Table 5(a-2)). Again, for the case of the developed shaving process, a large strain was generated in the tool cutting-edge vicinity and was decreased and directed toward the opposite side of the tool cutting-edge vicinity. However, the direction of this strain distribution was toward the shaved chip (Table 5(b-2).

The results showed that a large deformation that could readily facilitate crack formation was formed in the shearing zone in the case of the conventional shaving process. By contrast, the deformation was not formed in the shearing zone but was instead formed on the shaved chip in the case of the developed shaving process. These results confirmed that the developed

Table 5. Comparison of material flow and stress distribution analyses during shaving operation between conventional shaving die and proposed shaving die models.

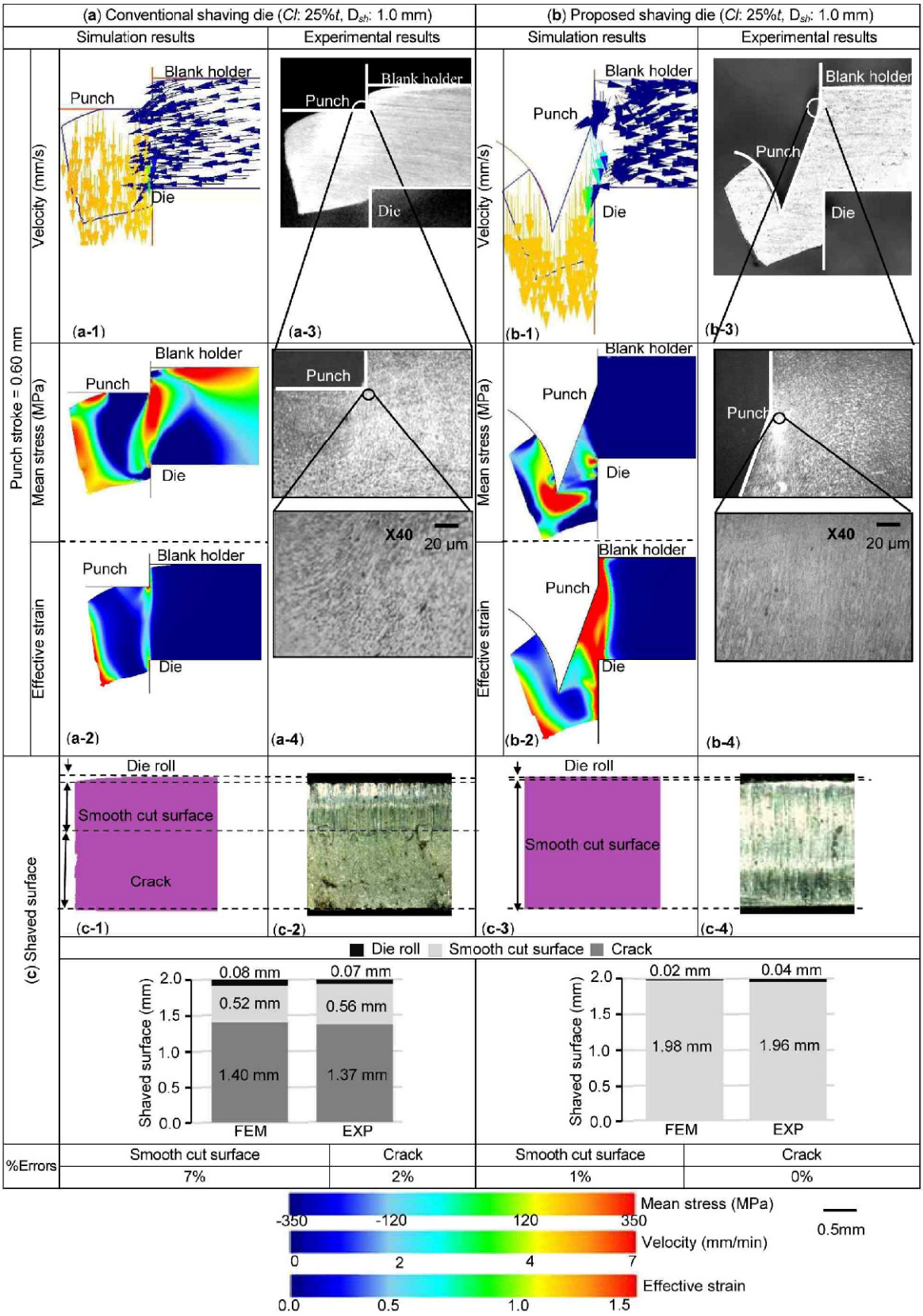

shaving die could be used to delay the crack formation in the shearing zone and that a smooth cut surface could be achieved. The experiments were also conduced and compared with the FEM simulation results in the cases of the conventional and developed shaving processes, as shown in Table 5(a-3) and (b-3), respectively. The FEM simulation results showed good agreement with the experimental results in terms of shaved-chip formation. The grain flow was also studied experimentally. In the case of the conventional shaving process, the microstructure of the grain flow showed an elongated grain around the cutting-edge vicinity (Table 5(a-4)), corresponded with the aforementioned material flow and stress distribution analyses. By contrast, for the case of the developed shaving process, the compressive stress was generated in the cutting-edge vicinity, as described in the aforementioned stress distribution analyses. The microstructure of the grain flow showed a fine elongated grain around the cutting-edge vicinity compared with that in the conventional shaving die model (Table 5(a-4)). These microstructure results indicated good correspondence with the FEM simulation results in addition to the shaved chip formation. After the shaving operation, the results showed that crack formation occurred in the case of the conventional shaving process by FEM simulation and experiment, as shown in Tables 5(c-1) and (c-2), respectively.

The FEM simulation results again showed good agreement for the die roll, smooth cut surface, and crack formation with the experimental results. For the case of the developed shaving process shown in Table 5(c-3) and (c-4) by FEM simulation and experiment, respectively, the results showed that crack formation could be prevented and that a smooth cut surface thorough the workpiece thickness could be achieved. The FEM simulation results were validated by experimental results. The FEM simulation results indicated good agreement of the predicted cut surface characteristics with the experimental results in the cases of the conventional and developed shaving processes (Table 5(c)). The die roll, smooth cut surface, and crack were also measured and reported. The errors of the FEM simulation compared with the experimental results in terms of the smooth cut surface and crack formation were generally less than 7 % and 1 % in the cases of the conventional and developed shaving processes, respectively. Based on the material flow and stress distribution analyses, a comparison of shaving mechanisms between the conventional and developed shaving processes is presented. The effects of the proposed punch geometry on the cut surface characteristics were investigated. Table 6 shows the stress and strain distribution analyses during shaving operation with respect to the cutting-edge angles. The larger the cutting-edge angle, the shorter the cutting side. Thus, prior to the cutting phase the larger the cutting-edge angle, the smaller the shaving allowance (Table 6(a)). Therefore, as the cutting-edge angle increased, the generated tensile stress on the rake tip and the generated compressive stress in the shearing zone decreased. Furthermore, the propagation of the stress distribution generated in the die cutting edge vicinity expanded into the shearing zone as the cutting-edge angle increased. The strain distribution also showed the same behavior as the stress distribution: The strain increasingly propagated into the shearing zone as the cutting-edge angle decreased (Table 6(a)). During the shaving phase, the generated tensile stress on the rake tip and die cutting-edge vicinity increased as the cutting stroke increased (Table 6(b)). The tensile stress generated in the die cutting-edge vicinity again increased and propagated into the shearing zone as the cutting-edge angle increased. However, this tensile stress and its propagation were obstructed by generating compressive stress in the shearing zone, which was formed by the cutting-edge angle. After compensating for these generated tensile and compressive stresses, the tensile stress could not be generated in the shearing zone in the case of a small cutting-edge angle (Table 6(b-1)).

By contrast, the stress was generated in the shearing zone in the case of a larger cutting-edge angle (Tables 6(b-2) and (b-3)). Furthermore, the generated tensile stress in the shearing zone was enlarged and increased as the cutting-edge angle increased. The strain distribution analysis is shown in Table 6(b). These analyses showed that the strain could be easily expanded and directed into a shaved chip when a small cutting-edge angle was applied. This process resulted in a crack readily being generated in the case of a small cutting-edge angle. As shown by these results, crack formation readily occurred when a large cutting-edge angle was applied. The shaved surface characteristics after the shaving operation are shown in Table 6(c). The results show that the entire smooth cut surface thorough the workpiece could be achieved in the cases of a small cutting-edge angle applied (Table 6(c-1)). By contrast, crack formation was observed in the case of large cutting-edge angles (Tables 6(c-2) and (c-3)). These results could be explained by the fact that in the case of a large cutting-edge angle, the generated compressive stress by cutting edge angle was insufficient to yield the tensile stress generated in the shearing zone during the shaving operation, and the crack formation could not be delayed. These experiments were also conducted to validate the FEM simulation results and are shown in Tables 6(c) and (d) in terms of the cut surface characteristics and cutting forces, respectively. The FEM simulation results agreed with the experimental results. The errors of the FEM simulation compared with the experimental results in terms of the smooth cut surface and crack formation were generally less than 7 %. In addition to the cut surface characteristics, the cutting force was observed to confirm the accuracy of the FEM simulation results, therein showing that the errors of the FEM simulation compared with the experimental results are approximately 6 %.

Table 7 shows the stress distribution analysis during shaving operation with respect to the cutting-edge widths. A larger cutting-edge width and a larger shaving allowance were used, and a larger compressive stress was generated underneath the cutting-edge angle and in the shearing zone (Table 7(a)). Next, during the shaving phase, the larger cutting-edge width resulted in the shaving allowance being easily forced down-

Table 6. Comparison of material flow and stress distribution analyses during shaving operation with respect to the cutting-edge angles (*C l*: 25 %*t*, D_{sh}: 1.0 mm, C_w: 0.8 mm, R_r: 2 mm).

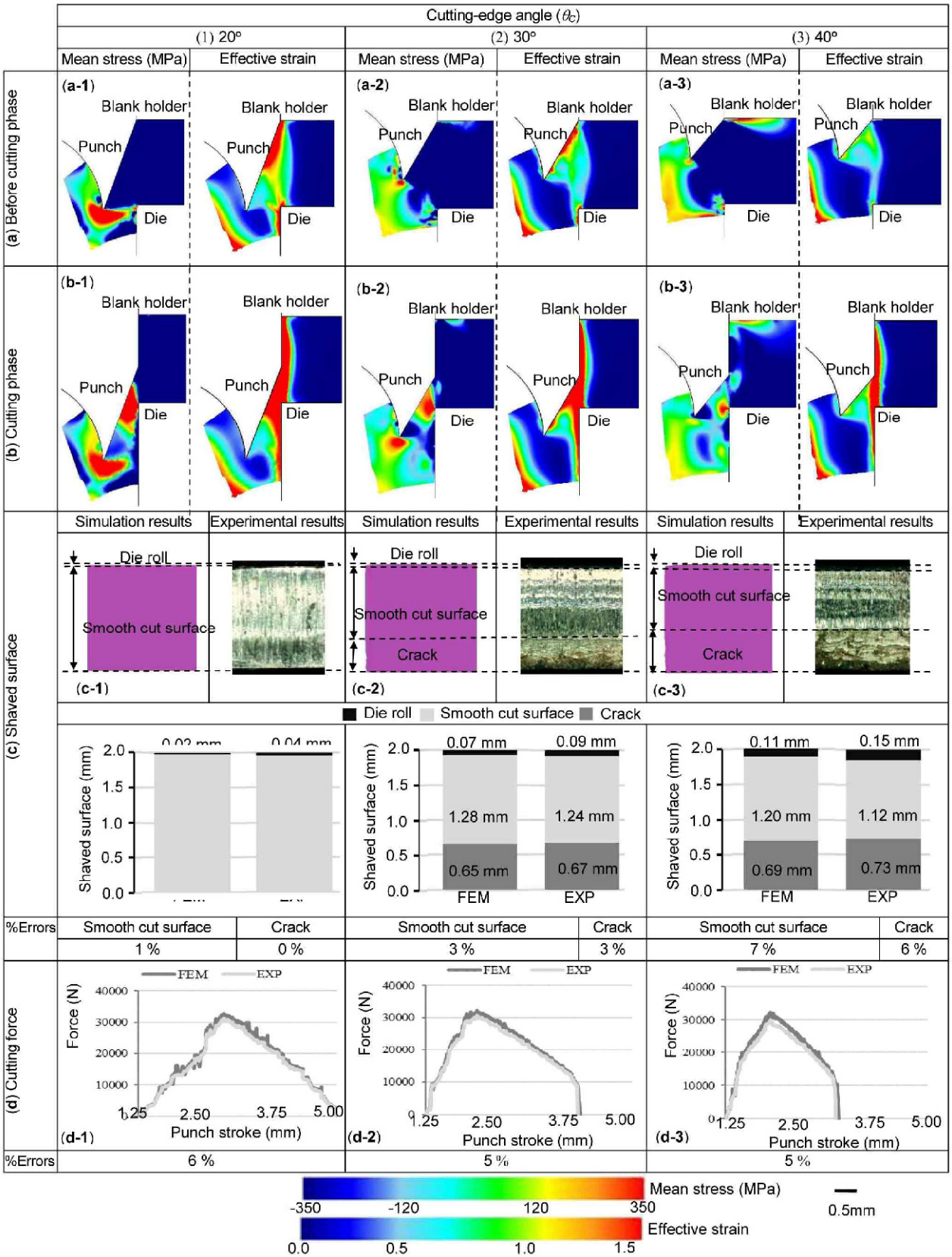

Table 7. Comparison of material flow and stress distribution analyses during shaving operation with respect to the cutting-edge widths (*C l*: 25 *%t*, D_{sh}: 1.0 mm, θ_C: 30°, R_i: 2 mm).

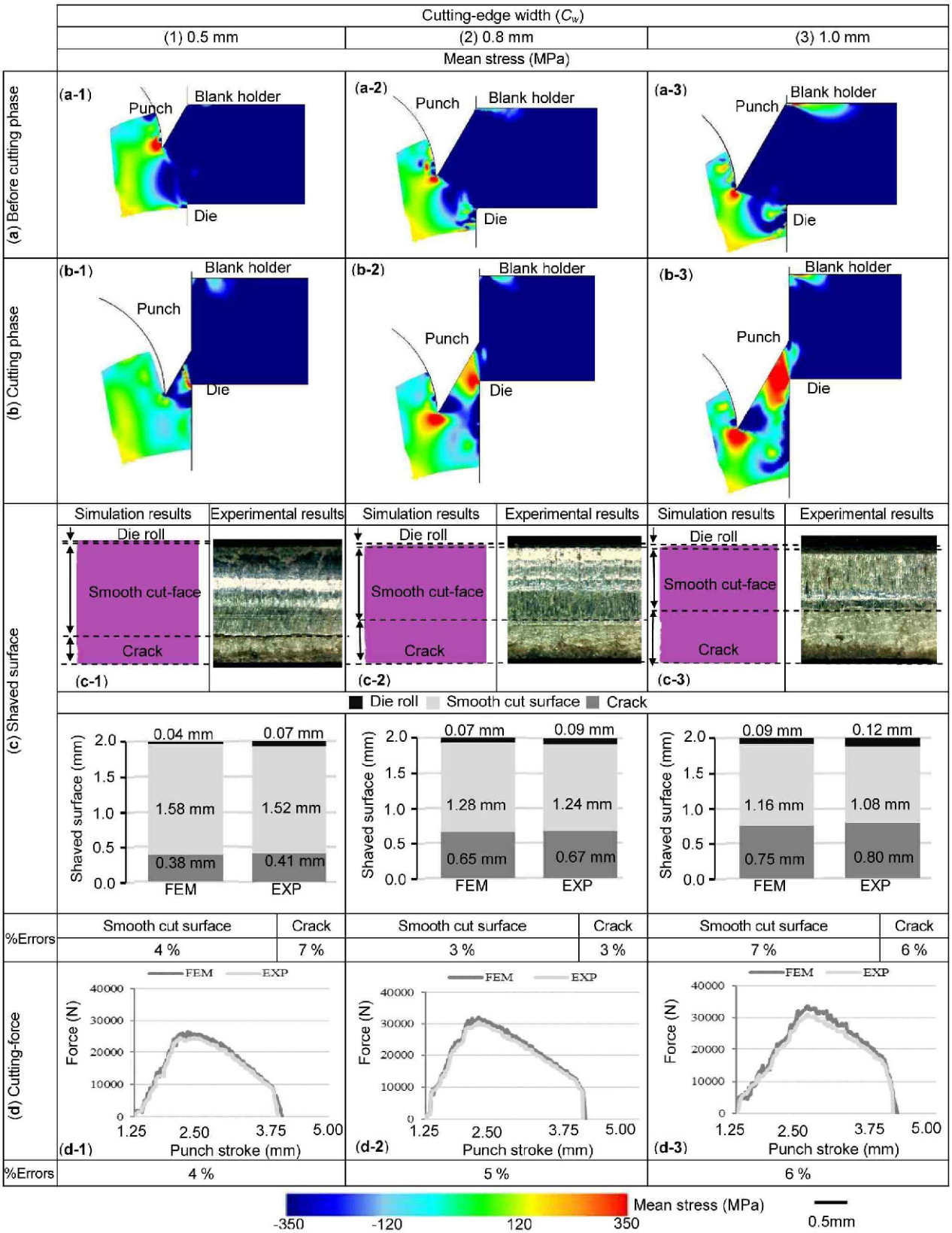

Table 8. Comparison of material flow and stress distribution analyses during shaving operation with respect to the rake radius (*Cl*: 25 *%t*, D_{sh}: 1.0 mm, θ_C: 20°, C_w: 0.8 mm).

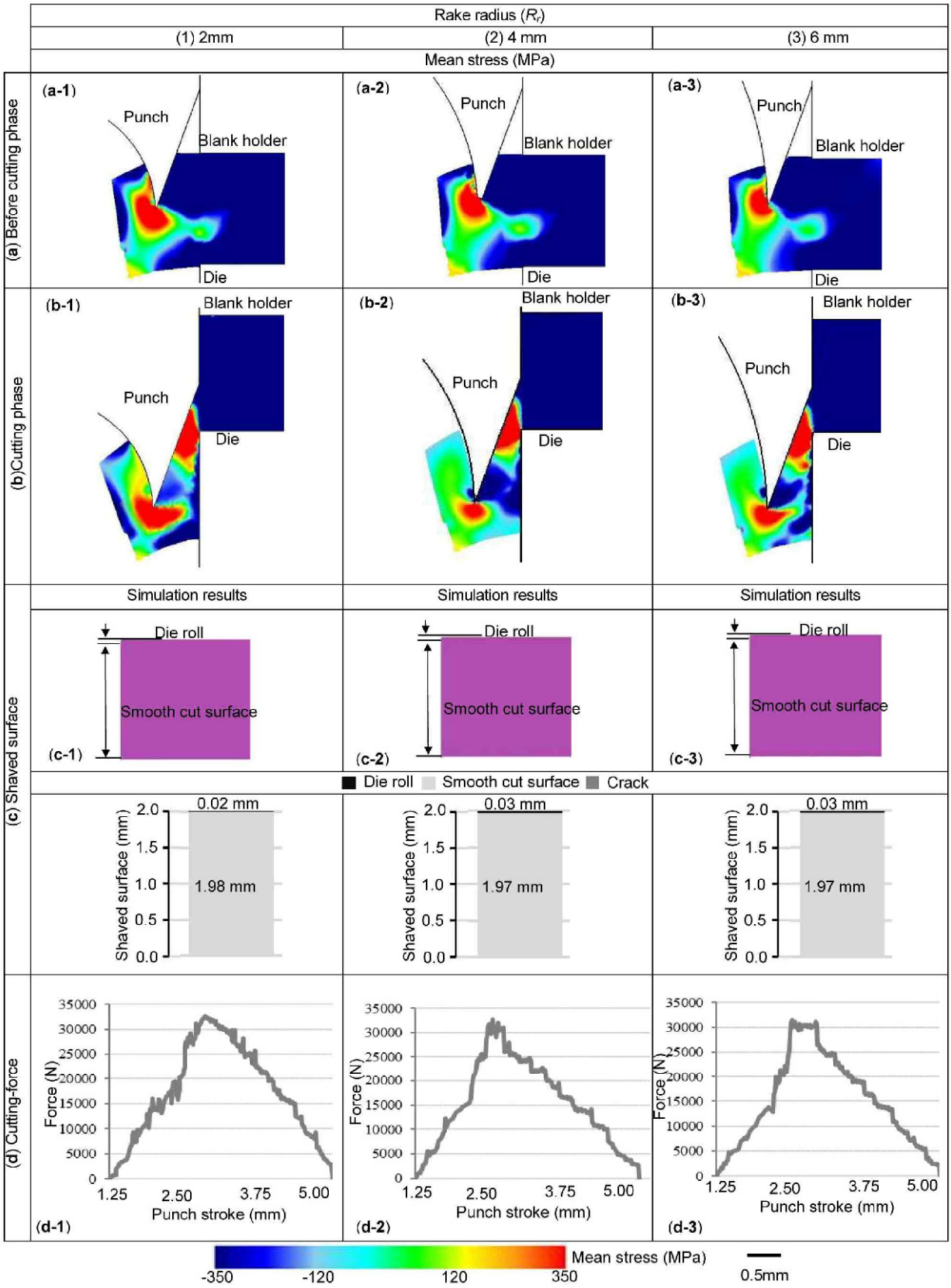

ward into the die, and the larger tensile stress was easily generated underneath the cutting edge angle and in the shearing zone (Table 7(b)). By compensating for these tensile and compressive stresses generated in the shearing zone, the compressive stress generated in the shearing zone decreased as the cutting-edge width increased. At the end of the shaving operation, the increases in the tensile stress during the cutting operation in the shearing zone overcame the generated compressive stress by the cutting side; the tensile stress was also larger than the fracture strength of the material and resulted in crack formation. Furthermore, the crack formation increased as the cutting-edge width increased (Table 7(c)). The FEM simulation results agreed with the experimental results in terms of shaved surface characteristics and cutting forces (Tables 7(c) and (d)). Table 8 shows the stress distribution analysis during shaving operation with respect to the rake radii. The results showed the same behavior as the stress distribution analysis with respect to the rake radii, as shown in Table 8(a). Specifically, the tensile stress was generated on the rake radius and the compressive stress generated underneath the cutting-edge angle. During shaving phase, the tensile stress generated in the shearing zone was compensated with compressive stress generated by the cutting-edge angle in all cases of rake radius (Table 8(b)). At the end of the shaving operation, the increases in the tensile stress during the shaving operation in the shearing zone could not overcome the fracture strength of the material, and crack formation could be delayed. After the shaving operation, the same shaved surface characteristics were obtained (Table 8(c)). Similar cutting forces were also predicted (Table 8(d)). As these results showed, the rake radius barely affected the cut surface characteristics and cutting force.

4. Conclusions

In the present study, the shaving process was improved to achieve smooth cut surface characteristics with a high-strength steel workpiece thickness. Conventional shaving process experiments were conducted to illustrate the shaved surface characteristics with respect to the process parameters and material types. The results elucidated that the use of a conventional shaving process could be successful for carbon steel and SPCC. However, it was not successful for high-strength steel, that is, SPFH590. In the present study, the causes of this problem were revealed. On the basis of the material flow, stress distribution, and strain distribution analyses, by comparing with the SPCC, the shaved chip underwent more difficulties in moving the punch face and caused increases in tensile stress generated in the cutting-edge vicinity, and cracks formed. To solve these problems, the developed punch shape with a cutting-edge angle and rake radius was proposed. First, to force the shaving allowance to move along the punch face and to prevent moving downward along the punch movement direction, the rake radius was designed to seperately tear off the shaving allowance and cause the shaved chip to be smaller. Thus, the torn-off shaving allowance was easily moved along the rake radius instead of moving downward along the punch movement direction; this process also delayed the increases in tensile stress generated in the cutting-edge vicinity and cracks. In addition to the rake radius, to decrease the high tensile stress generated in the cutting-edge vicinity and shearing zone, the cutting edge angle was designed to increase the generated compressive stress in the cutting-edge vicinity and shearing zone. On the basis of the two mechanisms of the developed shaving die, the generated tensile stress in the shearing zone could be delayed by compressive stress, and crack formation could be prevented. To validate the FEM simulation results, laboratory experiments were conducted. The experimental results agreed well with the FEM simulation results in terms of cut surface characteristics, including the die roll, smooth cut surface and crack formation. The cutting forces predicted by FEM simulation were also in agreement with those obtained by experiments. Furthermore, the effect of the punch geometry on the cut surface characteristics and cutting forces was investigated. The cutting-edge angle and width had strong effects on the changes in the stress distribution analysis generated in the shearing zone and on the shaved surface characteristics, but the rake radius was only weakly affected. Therefore, in the present study, a smooth cut surface thorough the workpiece thickness of high-strength steel, SPFH590, was achived using the developed shaving process.

Acknowledgments

This study was partially supported by Grants from The Thailand Research Fund under Grant No. RSA6180047 and The Higher Education Research Promotion and National Research University Project of Thailand, Office of the Higher Education Commission under Grant No. 57000618. The authors would also like to thank Miss Wiriyakorn Phanitwong, Ph.D. for her assistance during this study.

Nomenclature

θ_C	: Cutting-edge angle
R_r	: Rake radius
C_w	: Cutting-edge width
σ_u	: Tensile strength
δ	: Elongation
E	: Young's modulus
v	: Poisson's ratio
t	: Thickness
WP_L	: Workpiece length
WP_W	: Workpiece width
μ	: Friction coefficient
Cl	: Shearing clearance
D_{sh}	: Shaving allowance

References

[1] W. D. Thomas and K. Warse, Architecture for a neural expert system for condition-based maintenance of blanking, *International Journal of Materials and Product Technology,* 32 (4) (2007) 447-459.

[2] F. Djavanroodi, A. Pirgholi and E. Derakhshani, FEM and ANN analysis in fine-blanking process, *Materials and Manufacturing Processes,* 25 (2010) 864-872.

[3] P. L. Ship, Y. C. Dar and Y. L. Yeou, Relationship between the punch-die clearance and shearing quality of progressive shearing die, *Materials and Manufacturing Processes,* 25 (8) (2010) 786-792.

[4] S. Yiemchaiyaphum, M. Jin and S Thipprakmas, Die design in fine-piercing process by chamfering cutting edge, *Key Engineering Materials,* 443 (2010) 219-224.

[5] D. Peter, K. Thomas, G. Roland, V. Wolfram and H. Hartmut, Experimental investigation on the temperature distribution in the shearing zone during sheet metal blanking, *Steel Research International* (2012).

[6] A. T. Witthauer, G. Y. Kim, L. E. Faidley, Q. Z. Zou and Z. Wang, Effects of acoustic softening and hardening in high frequency vibration assisted punching of aluminum, *Materials and Manufacturing Processes,* 29 (2014) 1184-1189.

[7] D. Ri-Xian, G. Cheng, Z. Zi-Cai, Z. Ming-Kai and G. Rui-Peng, Piezoelectric-based non-destructive monitoring of contact pressures in fine-blanking process, *Journal of Engineering Manufacture,* 228 (8) (2014) 927-936.

[8] E. S. Abouel Nasr, H. M. A. Hussein, A. E. Ragab and A. K. Kamrani, A feature-based approach to an integrated CAD/CAPP system in sheet metal blanking dies, *International Journal of Rapid Manufacturing,* 4 (2014) 90-118.

[9] Y. Zhenming, B. Houssem, S. Khemais, Z. Xincun and G. Jun, Numerical simulation of sheet metal blanking based on fully coupled elastoplasticity-damage constitutive equations accounting for yield surface distortion-induced anisotropy, *International Journal of Damage Mechanics,* 26 (7) (2016) 1061-1079.

[10] A. Sontamino and S. Thipprakmas, Cut surface features in various die-cutting processes, *Key Engineering Materials,* 719 (2017) 127-131.

[11] C. Cristian, B. Philippe and P. P. Jean, On the numerical simulation of sheet metal blanking process, *International Journal of Material Forming,* 10 (2017) 55-71.

[12] B. Haohao, S. Hao, X. Ruili, C. Liping and Z. Zhiqiang, Finite element simulation of the punch with inclined edge in the sheet metal blanking process, *International Journal of Computing Science and Mathematics,* 9 (4) (2018) 377-389.

[13] W. Chung, K. Hwang, J. Kim and H. Ryu, A study on the improvement of the accuracy of a shaving process using a progressive die, *International Journal of Modern Physics B,* 22 (2008) 5673-5679.

[14] S. Thipprakmas, S. Rojananan and P. Paramaputi, An investigation of step taper-shaped punch in piercing process using finite element method, *Journal of Materials Processing Technology,* 197 (2008) 132-139.

[15] S. Thipprakmas and W. Phanitwong, Finite element analysis of shaving direction effects in reciprocating shaving process, *Steel Research International,* 81 (2010) 1058-1061.

[16] S. Thipprakmas, W. Phanitwong, M. Chinwithee and T. Morkprom, Reciprocating shaving approach to eliminate crack and burr formations in pressed parts, *Key Engineering Materials,* 443 (2010) 201-206.

[17] Y. Abe, Y. Okamoto, K. Mori and H. Jaafar, Deformation behaviour and reduction in flying speed of scrap in trimming of ultra-high strength steel sheets, *Journal of Materials Processing Technology,* 250 (2017) 372-378.

[18] K. Mori, Y. Abe and K. Sedoguchi, Deleyed fracture in cold blanking of ultra-high strength steel sheets, *Manufacturing Technology* (2019)

[19] T. Shiozaki, Y. Tamai and T. Urabe, Effect of residual stresses on fatigue strength of high strength steel sheets with punched holes, *International Journal of Fatigue,* 80 (2015) 324-331.

[20] Z. Cui, S. Bhattacharya, D. E. Green and A. T. Alpas, Mechanisms of die wear and wear-induced damage at the trimmed edge of high strength steel sheets, *Wear,* 426-426 (2019) 1635-1645.

[21] T. Matsuno, J. Nitta, K. Sato, M. Mizumura and M. Suehiro, Effect of shearing clearance and angle on stretch-flange formability evaluated by saddle-type forming test, *Journal of Materials Processing Technology,* 223 (2015) 98-104.

[22] A. Lara, I. Picas and D. Casellas, Effect of the cutting process on the fatigue behaviour of press hardened and high strength dual phase steels, *Journal of Materials Processing Technology,* 213 (2013) 1908-1919.

[23] K. Mori, Y. Abe, Y. Kidoma and P. Kadarno, Slight clearance punching of ultra-high strength steel sheets using punch having small round edge, *International Journal of Machine Tools and Manufacture,* 65 (2013) 41-46.

[24] H. Hongli, L. Huiping and H. Lianfang, Effect of technological parameters on microstructure and accuracy of B1500HS steel parts in the hot blanking, *International Journal of Advanced Manufacturing Technology,* 95 (2018) 3275-3287.

[25] K. Mori, Y. Abe, Y. Kidoma and P. Kadarno, Slight clearance punching of ultra-high strength steel sheets using punch having small round edge, *International Journal of Machine Tools and Manufactur,* 65 (2013) 41-46.

[26] W. Changsheng, C. Jun, Y. Xiangyu, X. Cedric and R. Feng, experimental investigations on wear resistance characteristics of different die materials for advanced high-strength steel blanking in close section, *Journal of Engineering Manufacture,* 228 (11) (2014) 1515-1525.

[27] W. Phanitwong, A. Sontamino and S. Thipprakmas, Experiment analysis of the feasibility of shaving process applied for high-strength steel sheet, *Advances in Materials Science and Engineering* (2016).

[28] Y. Chenjue, C. Jieshi, X. Cedric and Y. Xiangyu, Study of curvature and pre-damage effects on the edge stretch ability of advanced high strength steel based on a new simulation model,

International Journal of Material Forming, 9 (2016) 269-276.
[29] D. Son, H. Kim, J. Y. Kang, H. Y. Yun, J. J. Lee, S. K. Park, T. H. Lee and J. Lee, Analyses of the failures on shear cutting blades after trimming of ultra high-strength steel, *Engineering Failure Analysis,* 71 (2017)148-156.
[30] S. Thipprakmas and P. Wiriyakorn, Finite element analysis of flange-forming direction in the hole flanging process, *The International of Advanced Manufacturing Technology,* 61 (2012) 609-620.
[31] S. Thipprakmas, Application of Taguchi technique to investigation of geometry and position of V-ring indenter in fine-blanking process, *Materials and Design,* 31 (2010) 2496-2500.
[32] P. W. Myint, S. Hagihara, T. Tanaka, S. Taketomi and Y. Tadano, Determination of the values of critical ductile fracture criteria to predict fracture initiation in punching processes, *Journal of Manufacturing and Materials Processing,* 1 (2) (2017) 12.
[33] T. Intarakumthornchai, S. Jirathearanat, S. Thongprasert and P. Dechaumphai, FEA based optimization of blank holder force and pressure for hydromechanical deep drawing of parabolic cup using 2-D interval halving and RSM methods, *Engineering Journal,* 14 (2) (2010).
[34] M. P. Hong, W. S. Kim, J. H. Sung, D. H. Kim, K. M. B and Y. S. Kim, High-performance eco-friendly trimming die manufacturing using heterogeneous material additive manufacturing technologies, *International Journal of Precision Engineering and Manufacturing-Green Technology,* 5 (2017) 133-142.
[35] K. Lange, *Handbook of Metal Forming,* McGraw-Hill Inc., New York, USA, 24 (1985) 15.

Sutasn Thipprakmas, D.Eng., is a Professor at the Department of Tool and Materials Engineering at King Mongkut's University of Technology Thonburi, Thailand. His research interests include plastic deformation and metal forming process.

Arkarapon Sontamino is a Ph.D. candidate at the Department of Tool and Materials Engineering, King Mongkut's University of Technology Thonburi, Bangkok, Thailand.